Final Draft
of the original manuscript:

Napolitano, E.; Dolci, F.; Campesi, R.; Pistidda, C.; Hoelzel, M.; Moretto, P.;
Enzo, S. :

Crystal structure solution of KMg(ND)(ND2): An ordered mixed amide/imide compound

Crystal structure solution of KMg(ND)(ND$_2$): an ordered mixed amide/imide compound.

Emilio Napolitano[*,1], **Francesco Dolci**[1], **Renato Campesi**[1], **Claudio Pistidda**[2], **Markus Hoelzel**[3], **Pietro Moretto**[1], **Stefano Enzo**[4].

[1] *European Commission -DG Joint Research Centre-Institute for Energy and Transport, Westerduinweg 3, NL-1755 Petten, The Netherlands.*

[2]*Institute of Materials Research, Materials Technology, Helmholtz-Zentrum Geesthacht, Max-Planck-Straße 1, D-21502 Geesthacht, Germany.*

[3]*Forschungs Neutronenquelle Heinz Maier-Leibnitz (FRM II),Technische Universität München, Lichtenbergstrasse 1, D-85747 Garching, Germany.*

[4]*Dipartimento di Chimica e Farmacia, Università degli Studi di Sassari and INSTM, Via Vienna 2, I-07100 Sassari, Italy.*

*To whom correspondence should be addressed, email address:
emilio.napolitano@ec.europa.eu

ABSTRACT

An ordered mixed deuterated amide/imide potassium-magnesium compound was synthesized with the intent of solving its structure using neutron diffraction technique with help of "ab-initio" methods. Obtained powder diffraction patterns were compatible with the orthorhombic P2$_1$2$_1$2$_1$ space group, and lattice parameters a= 9.8896(3) Å; b = 9.3496(3) Å; c = 3.6630(1) Å, respectively. Assuming a density of 1.91 g/cm^3 the investigation has allowed to locate the four constituting elements distributed in seven different sites into Wyckoff general positions 4(a), for a total of 28 atoms in the unit cell. This is the first example of crystal structure solution of a mixed imide/amide compound appearing during the dehydrogenation process of a potassium containing amide based hydrogen storage material.

Keywords: Hydrogen storage; Hydrogen; Solid state; Crystal structure solution; Ab-initio methods; Powder diffraction.

1. INTRODUCTION

Solid state hydrogen storage offers the opportunity to address some of the issues associated with the use of a promising alternative energy vector such as gaseous hydrogen. Different materials have been investigated for such a purpose, and amide/hydride mixtures are among those giving best reversible performances, using relatively mild pressure/temperature conditions [1]. Different combinations of group I and II amides and hydrides have been tested, but the one giving the best compromise between kinetic performances, and hydrogen gravimetric content available at a temperatures around 200°C or lower, seems to be the Mg(NH$_2$)$_2$/2LiH mixture [2]. The enthalpy of formation for the Mg(NH$_2$)$_2$/2LiH system is in the order of 40 kJ/mol H$_2$, and its expected hydrogen equilibrium pressure at 90°C should be around 1bar [3]. Despite these features no significant hydrogen absorption/desorption kinetics can be recorded below 180°C. The simplest explanation for such behaviour is the presence of a kinetically controlled process associated with hydrogen absorption and release.

Many attempts have been made for improving the performances of $Mg(NH_2)_2/2LiH$ materials and lowering their working temperature [3]. Addition of potassium appears to significantly lower reaction temperatures [4]. Despite its positive effect on the hydrogen storage system, no specific role for potassium containing additives has been so far identified [5].

For mixed hydride/amide systems the occurrence of multiple reaction steps, involving intermediate phases, is well known and it was recognized in $LiH/LiNH_2$ [6, 7], $Mg(NH_2)_2/LiH$ [8] and CaH_2/LiH mixtures [9] respectively.

Understanding the specific nature and the role of different intermediates present inside magnesium amide/lithium hydride/potassium-doped systems, can offer relevant information on the fundamental mechanisms governing the good performances of these amide-based hydrogen storage materials.

Recently, Wang et al. [10] described the synthesis of a new mixed imide-amide phase $KMg(NH)(NH_2)$, appearing inside a hydrogen storage mixture composed by potassium hydride and magnesium amide. According to their work $KMg(NH)(NH_2)$ is the end product of the reversible dehydrogenation process of a $Mg(NH_2)_2/KH$ mixture.

Unfortunately the structure of such powdered compound was not determined. For such cases, where single crystals can not be grown, the powder diffraction techniques are the only suitable analytical tools to adopt for characterizing the compounds in solid state chemistry.

Generally, for new-unknown inorganic materials the knowledge of cell dimension, space group and inter-atomic connection are not known *a priori*. This lack of information makes it difficult the pathway towards a successful structure solution from powder diffraction data (SDPD).

Nevertheless, in this paper, we present a structural model for the potassium magnesium imide-amide powdered compound, $KMg(ND)(ND_2)$, previously synthesised by Wang et al. [10]. This crystal structure solution was carried out using the so called ab-initio methods [11]. By the use of neutron powder diffraction technique, starting from the hypothesis of a new unknown single phase and taking advantage of the initial chemical composition of the reagents as well as the spectroscopic infrared analysis by Wang et al. [10], we unambiguously show that amide and imide groups can coexist simultaneously inside the same phase. Our structural model helps in interpreting the results obtained by Wang et al. [10], and shows how structure relationships are necessary to better understand the reaction pathway for amide based systems.

2. EXPERIMENTAL METHODS AND NUMERICAL DATA ANALYSIS

Deuterated $KMg(ND)(ND_2)$ was synthetized using the methodology outlined in the paper by Wang et al. [10]. Deuterated potassium amide was produced by ball milling potassium deuteride (prepared by keeping potassium hydride under 20 bars of deuterium at 350°C for 12h) under 8 bars of deuterated ammonia. Magnesium deuteride was prepared by cycling magnesium hydride (Aldrich, hydrogen-storage grade) under deuterium atmosphere (Praxair, > 99%) at 350°C. Magnesium deuteride was subsequently ball milled under 8 bars of deuterated ammonia (Aldrich, 99% D atom).

Preliminary structural investigations were performed using a PANalytical Empyrean X-ray powder diffractometer in Bragg-Brentano geometry with Cu Kα radiation (λ=1.54178 Å). The X-ray generator worked at a power of 45 kV and 40 mA and the resolution of the instrument (divergent and antiscatter slits of 1°) was determined using LaB_6 standard (660a) free from the effect of reduced crystallite size and lattice defects [12]. The goniometer was equipped with a solid state real time multiple strip detector (RTMS) which gives the possibility of a fast data collection. The pattern was recorded in the angular range 10°-72° in 2θ, with a step scan of 0.04° and counting time of 1 s per point. The powder was spread onto a zero background, silicon single crystal specimen holder, and sealed in the glove-box with an air-tight hood of Kapton foil.

Neutron powder diffraction (NPD) experiments were performed using the high resolution powder diffractometer SPODI at the FRMII reactor source, Garching, Germany. The instrument is characterized by a very high monochromator take-off angle of 155° (standard configuration). The detector array consists of 80 ^{3}He position sensitive detector tubes (300 mm active height) with fixed Soller collimators of 10˙ horizontal divergence. The multidetector of SPODI spans an angular range of $2\theta = 160°$ as each detector covers 2° corresponding to 160° / 80 detectors. The data collection is performed via stepwise positioning of the detector array to obtain a diffraction pattern of the desired step width (typically 2°/40 steps resulting in $\Delta (2\theta) = 0.05°$).

The two-dimensional raw data are evaluated to provide diffraction patterns corresponding to different detector heights ranging from 10 mm to 300 mm and variable detector height, accounting for vertical beam divergence effects. Thus, asymmetric broadenings at quite low and high scattering angles are overcome, while the full detector height in the medium 2θ regime can be used. Further details of the diffractometer can be found [13].

Peak location was conducted using the X'Pert Highscore Program [14] and the indexing step using the McMaille [15] software supplemented with DICVOL06 [16] and N-TREOR [17] programs. Direct-Space Methods [18] were adopted in order to locate the atoms inside the unit cell. The simulated annealing program, Endeavour [19, 20] was employed and in addition, a parallel approach was carried out using FOX [21], EXPO2009 [22] and MAUD [23-25] programs.

Rietveld refinement (Fig 1-2) was performed using MAUD [23-25] software and crystal structure visualization using DIAMOND [26, 27] program.

In the course of the fit the instrument function of the diffractometer is convolved with the broadening function of the specimen under investigation. During the least squares refinement process the structure parameters, such as lattice parameters, atomic coordinates and temperature factors are optimized simultaneous to the microstructure parameters such as average crystallite size and lattice disorder.

3. Results

3.1 Structure solution.

The preliminary X-ray powder diffraction (XRPD) pattern (Fig.1) resembles closely the one attributed to the new amide/imide compound of potassium and magnesium by Wang et al. [10], even though an elevated background was present in their paper.

The neutron powder diffraction pattern collected for the deuterated compound is shown in Fig.2. NPD is essential for locating light atoms. This is due to the fact that for this technique the relative neutron scattering cross section [28] is N>D>Mg>K, while in the case of the X-rays the relative scattering factors series [28] reverses to K>Mg>N>H. Despite of this different sequence of comparative intensities, location of XRPD and neutron peaks are in good correspondence once reported on a d-scale.

Phase identification analysis was performed in order to identify crystalline phases. α-KNH$_2$ (PCD-1704966) [29-31] and MgO (COD-9000497) [32, 33] were recognized.

We were able to index the XRPD sequence of the first unassigned 20 peaks with a figure of merit (FoM) ≈ 20 [34] using a primitive orthorhombic cell with lattice parameters a = 9.891(4) Å; b = 9.343(4) Å; c = 3.660(3) Å respectively, and a cell volume Vc = 338.2(6) Å^3. Other successful cells

had volumes exactly 2, 3 and 4 times larger respectively (supercells), and their FoM was consequently lower. Very close results were returned after analysis of the first 20 reflexions selected from the neutron pattern. A FoM $\approx$ 37 was determined unambiguously according to a primitive orthorhombic cell with lattice parameters a = 9.882(2) Å; b = 9.344(2) Å and c = 3.660(1) Å respectively, and a cell volume V_c = 337.9(2) Å^3. The differences in the lattice parameter obtained with the two techniques can be due to a combination of various factors, such as the imperfect determination of the neutron wavelength after calibration, different instrument resolution, isotopic effects, and to different systematic zero offset values. The last potential source of uncertainty should be nearly absent in a neutron diffractometer when carried out in transmission but may occur in a Bragg-Brentano parafocusing geometry. Any difference between the two patterns should be evaluated after the refinement stage.

3.2 Density assumption

In the absence of experimental density measurements some considerations seem appropriate. Assuming that the chemical composition of the new phase is $KMg(ND)(ND_2)$, as it was suggested by Wang et al. [10] on the basis of spectroscopic infrared (IR) evidence and weight measurements, its orthorhombic cell is likely to host Z = 4 asymmetric units, leading to a calculated density of 1.91 g/cm^3 (1.85 g/cm^3, for the non-deuterated compound) This is nearly the density measured by Jacobs and Juza for MgNH (1.827 g/cm^3) [35] and obtained recently after solving the structure of magnesium imide MgND with a P6/m space group [36].

For comparison, the calculated and measured density of di-potassium magnesium tetra-amide $K_2Mg(NH_2)_4$ with the monoclinic structure S. G. $P2_1/c$ reported by Jacobs et al. [37] shows a density of 1.62 g/cm^3. Moreover the four polymorphs known for potassium amide KNH_2 show a density varying from 1.59 to 1.66 g/cm^3 [38, 39]. On the other hand $KNH_2 \cdot NH_3$ holds a density of 1.894 g/cm^3 [40] while for $KNH_2 \cdot 2NH_3$ it holds 1.321 g/cm^3, respectively [41].

Unfortunately the structures of the potassium magnesium double imide $K_2Mg(NH)_2$ and of another di-potassium magnesium amide/imide compound of formula $K_2Mg(NH_2)_2(NH)$ have not been determined, nor their densities were measured [42, 43].

Though our estimated density for an amide/imide compound appears relatively high, it remains the most plausible value. Using Endeavour [19, 20], after scanning the primitive orthorhombic symmetries, the best solution for both X-ray and neutron diffraction patterns was achieved using the space group n. 19 ($P2_12_12_1$), where the atoms are all located in 4(a) general positions. The outcome of the final refinement process is shown in Figures 1-2, giving lattice parameters and atomic coordinates as are reported in Table 1-2. In this concluding stage some small differences in the lattice parameters evaluation from indexing step are present. This depends from the peak positions (including their uncertainty) and from the specific algorithm used by each indexing software (e.g., DICVOL06 vs McMaille or N-TREOR). We should also consider that, after the refining stage, the relative peak intensities and the shape of peaks are actually taken into account in addition to the mere peak position values.

4. Discussion

$KMg(ND)(ND_2)$ is a compound with a structure able to accommodate together features from different families of alkali and alkali metal earth imides and amides, each one with their peculiar and specific features (Fig.3). Each Mg experiments a tetrahedral coordination environment by three N1 atoms (imide ND^{2-} ions) with Mg-N1 distances ranging from 2.088(2) Å to 2.104(7) Å, and one N2 (amide ND_2^- unit) with distance Mg-N2 2.059(1) Å (Fig. 4). The angles range from 94.99(1) ° to 121.18(5) °, showing a significant deviation from the ideal tetrahedral geometry. Each MgN$_4$ is linked to other two adjacent tetrahedra *via* two edges and three N1 atoms at the respective vertices. This leads to an infinite cis-edge-sharing [Mg-N1] tetrahedra chain of $[Mg(N1D)_3N2D_2]_n$ running

parallel along [001] direction (Fig.5). The fourth nitrogen corner is occupied by N2 atom of the ND_2^- fragment. The magnesium-nitrogen distances for MgN_4 tetrahedra in $KMg(ND)(ND_2)$ are about 2.06Å, 2.09Å, 2.10Å and 2.11Å, respectively. The present crystal structure model shows differences in magnesium-nitrogen bond lengths with respect to $K_2Mg(NH_2)_4$ compound, wherein the Mg-N distances in MgN_4 tetrahedra are around 2.04Å, 2.05Å, 2.08Å and 2.09Å, respectively. It is evident that magnesium-nitrogen distances in $KMg(ND)(ND_2)$ are closer to the ones of MgND [36]. Similar values for the closest magnesium-magnesium distances are obtained for $KMg(ND)(ND_2)$ (2.84Å) and MgND (2.79Å).

Also, the two nitrogen atoms adopt a tetrahedral coordination geometry surrounded by a different chemical environment.
The N1 atom is tetrahedrally coordinated by three Mg atoms and one D1 atom forming a distorted tetrahedron (Fig.6), its Mg-N distances ranging from 2.088(2) Å to 2.104(7) Å, N1-D1 distance value of 0.987(7) Å, and its angles varying from 107.70(6)° to 140.21(2)°. Each distorted tetrahedron shares two magnesium corners and three edges, with two adjacent tetrahedra leading to an infinite cis-share-edge chain of $[N1Mg_3D1]_n$ along the c-axis.

The arrangement of the two different type of tetrahedra, $[Mg(N1D1)_3N2D_2]$ and $[N1Mg_3D1]$, gives rise to an inter-penetrating tetrahedral packing ···TtT··· type of two chains along [001] direction (Fig.7).

The N2 of the ND_2^- unit is also tetra-coordinated by Mg, K atoms and two deuterium ones, D2 and D3 respectively. The bond lengths of N2-D2 and N2-D3 are respectively 0.960(6) Å and 1.042(5) Å, however N2-Mg and N2-K are 2.059(1) Å and 2.889(2) Å.

The potassium cations adopt a heptahedral coordination sphere by nitrogen atoms forming a trigonal prismatic mono-capped polyhedron (Fig.8). Potassium-nitrogen distances for the KN_7 in $KMg(ND)(ND_2)$ are approximately 2.89Å, 2.93Å, 3.06Å, 3.09Å, 3.11Å, 3.38Å and 3.40 Å. This compares well with potassium-nitrogen distances in $K_2Mg(NH_2)_4$, where distances are approximately 2.85Å, 2.86Å, 2.94Å, 3.02Å, 3.10Å, 3.32 Å and 3.4 Å. Similar distances between the two nearest potassium atoms are obtained in $KMg(ND)(ND_2)$ (3.66Å) and $K_2Mg(NH_2)_4$ (3.68Å).
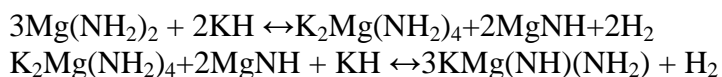
A remarkable peculiarity of $KMg(ND)(ND_2)$ is the presence of imide groups bonded to potassium cations. At present no pure inorganic potassium imide phase is known, and $KMg(ND)(ND_2)$ offers for the first time evidence for the occurrence of a potassium-containing compound associated to imide ND^{2-} groups.

The N-D distance in the imide fragment ND^{2-} is 0.988 Å, while in the amide $D-N-D^-$ molecular fragment there is an asymmetrical behaviour with N-D2 = 0.96 Å and N-D3 1.04 Å distances, respectively. These values are comparable with those determined by Sørby et al [44] for $Mg(ND_2)_2$ compound. The rather unusual fact of course relates to the high calculated density. The $Mg···$ -NH_2 distance of 2.06Å is certainly shorter than the K-NH_2 distance of 2.91 Å, but also slightly shorter than 2.09Å for the Mg-NH distance formally involved in the imide group. It will be interesting to account for these data in the correspondent FT-IR spectra and/or using a computational energy minimization approach.

The two crystal structures of $KMg(ND)(ND_2)$ and $K_2Mg(NH_2)_4$ are related to each other. Both compounds can be described as a combination of hepta-coordinated potassium ions (KN_7) forming linear chains by sharing one face, and magnesium-nitrogen MgN_4 tetrahedra. The arrangement of these building units is different in both structures, with a more dense packing of potassium inside the $K_2Mg(NH_2)_4$ structure, where KN_7 forms linear chains of two face-sharing among polyhedra, while in $KMg(NH)(NH_2)$ KN_7 polyhedral chains share only one face and one edge among each other (Fig. 9-10). The larger space available in between potassium linear chains in the crystal structure of $KMg(ND)(ND_2)$ is filled by a higher quantity of magnesium cations.

In both cases hydrogen/deuterium atoms are inside linear channels with a parallelogram section. In the case of KMg(ND)(ND$_2$) the D atoms of imide ND^{2-} and amide DND$^-$ anions are pointing to the centre of the channel, with ND^{2-} and DND$^-$ units located in opposite vertices (N1-N1 and N2-N2 distances 8.9664(9) Å and 4.2721(1) Å, respectively) . For K$_2$Mg(NH$_2$)$_4$ two sides of the channel are defined by MgN$_4$ tetrahedra and two by KN$_7$ polyhedra, while for KMg(ND)(ND$_2$) all the four sides of the channels are defined by KN$_7$ edges (N-N 6.594(1) Å and 4.093(2) Å respectively).

As for the mechanism of formation of the new imide/amide phase, it is interesting to recall the observation of Wang et al. [10] regarding the presence of two different reaction pathways depending on the reaction time allowed for equilibrium with the hydrogen atmosphere, after analysis of dehydrogenation curves. The reaction pathway is supposed to follow a two-steps mechanism:

$$3Mg(NH_2)_2 + 2KH \leftrightarrow K_2Mg(NH_2)_4 + 2MgNH + 2H_2$$
$$K_2Mg(NH_2)_4 + 2MgNH + KH \leftrightarrow 3KMg(NH)(NH_2) + H_2$$

Wang et. al[10] reported that the reaction actually proceeds at 190°C with a duration time of 3 h under near-equilibrium condition in one step as it follows:

$$Mg(NH_2)_2 + KH \leftrightarrow KMg(NH)(NH_2) + H_2$$

The presence of a time-dependent reaction pathway, hints to the existence of a crucial rate limiting step. Since a K$_2$Mg(NH$_2$)$_4$/MgNH mixture transforms into the KMg(NH)(NH$_2$) phase only after thermal treatment above 190 °C and time longer than 3 hours, it is reasonable to assume that the thermodynamic stable state involves the formation of KMg(NH)(NH$_2$). This is an evidence for a thermally activated process entailing migration or significant rearrangement of ions. Presence of magnesium imide (MgNH) is observed as intermediate only when thermodynamic equilibrium conditions are not reached [10], while in the most thermodynamic stable compound KMg(NH)(NH$_2$), imide groups are coexisting together with a amide groups in the same phase.

It is likely that, during the dehydrogenation process, magnesium atoms have to be accommodated inside a K$_2$Mg(NH$_2$)$_4$ structure which is already quite stable. Diffusion of doubly charged magnesium cations, or rearrangement of KN$_7$ linear chains are likely to be a slow process with high thermal energy barrier. The presence of a preferential bonding of magnesium ions with imide groups is retained inside the KMg(NH)(NH$_2$) structure. Magnesium atoms are bonded to three imide groups and just one amide group, while potassium cations are coordinated by four amide groups and three imide groups.

In a whole, the coexistence of amide and imide groups can be crucial in designing better hydrogen storage materials. Having a clear structural model for a thermodynamically stable, but kinetically hindered intermediate can help in elucidating some of the recent experimental findings for mixed amide-hydride hydrogen storage mixtures. Presence of channels and cavities were also evidenced suggesting areas where atoms/molecules can diffuse and exchange with the atmosphere. Such cavities can increase the internal surface of bulk material, which decreasing the effects associated with sintering, and contributing to the total surface area experimented by hydrogen molecules [45]. The new crystal structure can be related to those of the following hydrogenation intermediates [8]. Before a complete hydrogenated material (amide plus hydride) is formed, the starting compound goes through a series of intermediated steps [6, 9, 46, 47]. The stabilities of these intermediate phases is directly associated to the hydrogen activity that the systems is subjected [48] The coexistence of anions with different charges which can be converted into each other allows for the accommodation of defects, and helping in achieving charge neutrality more easily. The N-D2 in ND$_2^-$ groups may have different N-D bond length compared to N-D3[44].

5. Conclusions

This work shows in uncontroversial manner the crystal structure solution for a likely thermodynamically stable, but kinetically hindered intermediate phase occurring in a mixed imide-amide potassium magnesium powdered composite, $KMg(ND)(ND_2)$. The $KMg(ND)(ND_2)$ compound is able to accommodate together imides and amides groups interacting with magnesium atoms in tetrahedral coordination, and showing for the first time a potassium imide/amide heptahedral geometry arrangement.

Our symmetry and relative intensity analysis suggested the orthorhombic $P2_12_12_1$ space group n. 19. Precise location of deuterium atoms was possible because the use of neutron diffraction pattern. The four constituent species, are distributed in seven different sites located in 4 (a) Wyckoff positions, for a total of 28 atoms inside the unit cell, with a calculated density of 1.85 g/cm^3 for the non-deuterated compound.

Some additional special aspects of the $KMg(ND)(ND_2)$ structure deserve further considerations:

- The presence of channels and cavities can promote enhanced gas diffusion and gas-matter exchange paths. This internal surface could therefore counterbalance the surface decrease associated with sintering.

- The coexistence of anions with different charges which can be converted into each other allows for the accommodation of defects, and helps in achieving charge neutrality more easily. The imide N-D interatomic distance holds 0.987 Å, close to the value determined in single phase MgND compound, and in the amide groups the coordinates of D atoms are suggesting different N2-D2 ≈ 0.960 Å and N2-D3 ≈ 1.042 Å distance values, respectively. Imide and amide units can be considered as anions with different partial charges on hydrogen atoms, like in the case, even if less extreme, of BH_4^- and NH_2^- groups.

The demonstrated coexistence of amide and imide groups could assist in future designing better and advanced hydrogen storage materials.

References

[1] Gregory DH. Lithium Nitrides, Imides and Amides as Lightweight, Reversible Hydrogen Stores. J Mater Chem. 2008; 18:2321-30.

[2] Lohstroh W, Fichtner M. Reaction steps in the Li–Mg–N–H hydrogen storage system. Journal of Alloys and Compounds. 2007;446–447:332-5.

[3] Xiong Z, Hu J, Wu G, Chen P, Luo W, Gross K, et al. Thermodynamic and kinetic investigations of the hydrogen storage in the Li–Mg–N–H system. Journal of Alloys and Compounds. 2005;398:235-9.

[4] Wang J, Liu T, Wu G, Li W, Liu Y, Araújo CM, et al. Potassium-Modified Mg (NH2) 2/2 LiH System for Hydrogen Storage. Angewandte Chemie International Edition. 2009;48:5828-32.

[5] Luo W, Stavila V, Klebanoff LE. New insights into the mechanism of activation and hydrogen absorption of (2LiNH2–MgH2). International Journal of Hydrogen Energy. 2012;37:6646-52.

[6] David WIF, Jones MO, Gregory DH, Jewell CM, Johnson SR, Walton A, et al. A Mechanism for Non-stoichiometry in the Lithium Amide/Lithium Imide Hydrogen Storage Reaction. Journal of the American Chemical Society. 2007;129:1594-601.

[7] Weidner E, Bull DJ, Shabalin IL, Keens SG, Telling MTF, Ross DK. Observation of novel phases during deuteration of lithium nitride from in situ neutron diffraction. Chemical Physics Letters. 2007;444:76-9.

[8] Weidner E, Dolci F, Hu J, Lohstroh W, Hansen T, Bull DJ, et al. Hydrogenation Reaction Pathway in $Li_2Mg(NH)_2$. The Journal of Physical Chemistry C. 2009;113:15772-7.

[9] Wu H. Structure of Ternary Imide Li2Ca(NH)2 and Hydrogen Storage Mechanisms in Amide−Hydride System. Journal of the American Chemical Society. 2008;130:6515-22.

[10] Wang J, Wu G, Chua YS, Guo J, Xiong Z, Zhang Y, et al. Hydrogen Sorption from the Mg(NH2)2-KH System and Synthesis of an Amide–Imide Complex of KMg(NH)(NH2). ChemSusChem. 2011;4:1622-8.

[11] Harris KDM, Tremayne M, Kariuki BM. Contemporary Advances in the Use of Powder X-Ray Diffraction for Structure Determination. Angewandte Chemie International Edition. 2001;40:1626-51.

[12] Enzo S, Fagherazzi G, Benedetti A, Polizzi S. A profile-fitting procedure for analysis of broadened X-ray diffraction peaks. I. Methodology. Journal of Applied Crystallography. 1988;21:536-42.

[13] Hoelzel M, Senyshyn A, Juenke N, Boysen H, Schmahl W, Fuess H. High-resolution neutron powder diffractometer SPODI at research reactor FRM II. Nuclear Instruments and Methods in Physics Research Section A: Accelerators, Spectrometers, Detectors and Associated Equipment. 2012;667:32-7.

[14] PANalytical. X'pert Data Collector and X'pert Highscore. PANalytical BV, Almelo, The Netherlands. 2003.

[15] Le Bail A. Monte Carlo indexing with McMaille. Powder Diffraction. 2004:249-54.

[16] Boultif A, Louer D. Powder pattern indexing with the dichotomy method. Journal of Applied Crystallography. 2004;37:724-31.

[17] Altomare A, Giacovazzo C, Guagliardi A, Moliterni AGG, Rizzi R, Werner P-E. New techniques for indexing: N-TREOR in EXPO. Journal of Applied Crystallography. 2000;33:1180-6.

[18] Černý R, Favre-Nicolin V. Direct space methods of structure determination from powder diffraction: principles, guidelines and perspectives. Zeitschrift für Kristallographie. 2007;222:105-13.

[19] Endeavour. -Structure Solution from Powder Diffraction. -Crystal Impact - Dr. H. Putz & Dr. K. Brandenburg, ;GbR, Kreuzherrenstr. 102, 53227 Bonn, Germany.

[20] Putz H, Schon JC, Jansen M. Combined method for ab initio structure solution from powder diffraction data. Journal of Applied Crystallography. 1999;32:864-70.

[21] Favre-Nicolin V, Cerny R. FOX, `free objects for crystallography': a modular approach to ab initio structure determination from powder diffraction. Journal of Applied Crystallography. 2002;35:734-43.

[22] Altomare A, Camalli M, Cuocci C, Giacovazzo C, Moliterni A, Rizzi R. EXPO2009: structure solution by powder data in direct and reciprocal space. Journal of Applied Crystallography. 2009;42:1197-202.

[23] Lutterotti L. The MAUD Program, http://www.ing.unitn.it/~luttero/maud.

[24] Lutterotti L, Matthies S, Wenk HR, Schultz AS, Richardson JW. Combined texture and structure analysis of deformed limestone from time-of-flight neutron diffraction spectra. Journal of Applied Physics. 1997;81:594-600.

[25] Wenk HR, Lutterotti L, Vogel SC. Rietveld texture analysis from TOF neutron diffraction data. Powder Diffraction. 2010;25:283-96.

[26] Diamond. - Crystal and Molecular Structure Visualization. Crystal Impact - Dr. H. Putz & Dr. K. Brandenburg GbR , Kreuzherrenstr. 102, 53227 Bonn, Germany.

[27] Pennington WT. DIAMOND-Visual crystal structure information system. Journal of Applied Crystallography. 1999;32:1028-9.

[28] International Tables for Crystallography, vol. C, (2006). E Prince, Ed Published by Springer and International Union of Crystallography (IUCr)

[29] Juza R, Jacobs H, Klose W. Die Kristallstrukturen der Tieftemperaturmodifikationen von Kalium- und Rubidiumamid. Zeitschrift für anorganische und allgemeine Chemie. 1965;338:171-8.

[30] Villars P, Cenzual K. Pearson's Crystal Data, Crystal Structure Database for Inorganic Compounds. Materials Park (OH): ASM International. 2013.

[31] Pearson's Crystal Data - Crystal Structure Database for Inorganic Compounds - Crystal Impact - Dr. H. Putz & Dr. K. Brandenburg GbR , Kreuzherrenstr. 102, 53227 Bonn, Germany.

[32] Grazulis S, Chateigner D, Downs RT, Yokochi A, Quirós M, Lutterotti L, et al. Crystallography Open Database-an open-access collection of crystal structures. Journal of Applied Crystallography. 2009;42:726-9.

[33] Hazen R, M. Effects of temperature and pressure on the cell dimension and X-ray temperature factors of periclase. American Mineralogist. 1976;61:266-71.

[34] de Wolff PM. A simplified criterion for the reliability of a powder pattern indexing. Journal of Applied Crystallography. 1968;1:108-13.

[35] Jacobs H, Juza R. Darstellung und Eigenschaften von Magnesiumamid und -imid. Zeitschrift für anorganische und allgemeine Chemie. 1969;370:254-61.

[36] Dolci F, Napolitano E, Weidner E, Enzo S, Moretto P, Brunelli M, et al. Magnesium Imide: Synthesis and Structure Determination of an Unconventional Alkaline Earth Imide from Decomposition of Magnesium Amide. Inorganic Chemistry. 2010;50:1116-22.

[37] Jacobs H, Birkenbeul J, Kockelkorn J. Darstellung und eigenschaften der amidomagnesate des kaliums und rubidiums K2[Mg(NH2)4]- und Rb2[Mg(NH2)4]-Verbindungen mit isolierten [Mg(NH2)4]2−-tetraedern. Journal of the Less Common Metals. 1984;97:205-14.

[38] Juza R, Jacobs H, Klose W. Die Kristallstrukturen der Tieftemperaturmodifikationen von Kalium-und Rubidiumamid. Zeitschrift für anorganische und allgemeine Chemie. 1965;338:171-8.

[39] Juza R, Liedtke H. Zur Kenntnis des Kaliumamids. Zeitschrift für anorganische und allgemeine Chemie. 1957;290:205-8.

[40] Peters D, Tenten A, Jacobs H. Wasserstoffbrückenbindungen in den Monoammoniakaten von Kalium- und Caesiumamid. Zeitschrift für anorganische und allgemeine Chemie. 2002;628:1521-4.

[41] Kraus F, Korber N. Hydrogen Bonds in Potassium Amide-Ammonia(1/2), KNH2·2NH3. Zeitschrift für anorganische und allgemeine Chemie. 2005;631:1032-4.

[42] Palvadeau P, Rouxel J. Fr J, Bull Soc Chim. 1970:480-5.

[43] Palvadeau P, Rouxel J. C R Seances Acad Sci Ser C. 1968:1605 – 7.

[44] Sørby MH, Nakamura Y, Brinks HW, Ichikawa T, Hino S, Fujii H, et al. The crystal structure of LiND2 and Mg(ND2)2. Journal of Alloys and Compounds. 2007;428:297-301.

[45] Borgschulte A, Jones MO, Callini E, Probst B, Kato S, Züttel A, et al. Surface and bulk reactions in borohydrides and amides. Energy & Environmental Science. 2012;5:6823-32.

[46] Crivello JC, Gupta M, Černý R, Latroche M, Chandra D. Density functional study of Li_4NH and $Li_{1.5}NH_{1.5}$ as intermediary compounds during hydrogenation of Li_3N. Physical Review B. 2010;81:104113.

[47] Rijssenbeek J, Gao Y, Hanson J, Huang Q, Jones C, Toby B. Crystal structure determination and reaction pathway of amide–hydride mixtures. Journal of Alloys and Compounds. 2008;454:233-44.

[48] Daniel J. Bull EW, Igor L. Shabalin , Mark T. F. Telling , Catherine M. Jewell , Duncan H. Gregory and D. Keith Ross Pressure-dependent deuterium reaction pathways in the Li–N–D system. Physical Chemistry Chemical Physics 2010;12:2089-97.

Figure captions

Figure 1. The X-ray powder pattern of the new amide-imide phase (small blue dots) is described in terms the Rietveld approach (full red line) with the contribution of a new orthorhombic phase as described in the text, The bar sequences are related to the peak positions expected for each phase. The bottom line represents the residual curve. Rwp: 0.1166; Space Group $P2_12_12_1$ (n. 19); Z = 4; X-rays: $CuK\alpha_{1,2}$; λ = 1.5418 Å. This solution was possible mainly because the powder specimen is nearly single phase, apart from some minor by-products that were evaluated more accurately from the corresponding neutron pattern of the deuterated compound.

Figure 2. The neutron powder pattern. The experimental data points were described in terms of a new orthorhombic phase plus two further weaker components attributed to MgO and **α-**KNH_2 respectively. λ = 1.5482 Å; Rwp: 0.0355.

Figure 3. Unit-cell content view of the $KMg(ND)(ND_2)$. The 28 atoms are located in 4(a) Wyckoff sites. It is possible to evaluate the presence of imide/amide groups.

Figure 4. Coordination view of Mg^{2+} cation. Three ND^{2-} and one ND_2^- ions are bound to Mg^{2+} in a tetrahedral conformation.

Figure 5. (top) infinite chains of cis-edge sharing $[Mg(N1D)_3N2D_2]$ tetrahedra running along [001] direction. (bottom) A perspective projection of $KMg(ND)(ND_2)$ cell packing along c axis.

Figure 6. Distorted tetrahedral coordination of N1 and N2 atoms are shown.

Figure 7. Cell content view of $KMg(ND)(ND_2)$. The tetrahedra $[MgN_4]$ (purple) and $[N1Mg_3D1]$ (turquoise) are shown.

Figure 8. Potassium heptahedral chemical environment here is reported (top). Three ND^{2-} and four ND_2^- anion units surround the central K^+ cation. K-D distances (< 3 Å) are shown. Trigonal prism mono-capped KN_7 is shown in purple. The 7th ligand (ND^{2-}) is located on the top of the rectangular face of the trigonal prism (bottom figure).

Figure 9. Polyedral rappresentation of $KMg(ND)(ND_2)$ down to the [001] direction. Trigonal prisms mono-capped KN_7 (purple) and tetrahedra MgN_4 (yellow) are shown.

Figure 10. Projection view along the (100) direction of $K_2Mg(NH_2)_2$.

Tables caption

Table 1. Fractional atomic coordinates and isotropic displacement parameters of titled compound, $KMg(ND)(ND_2)$, achieved after Rietveld refinement of room temperature NPD.

Table 2. Cell parameters values obtained after X-ray an NPD Rietveld refinement. The difference in significant digits comes from the different number of hkl reflections made available by the two patterns, NPD 540 hkl vs PXRD 146 hkl, respectively.